

Electrically Active Defects Induced by α -Particle Irradiation in p-Type Si Surface Barrier Detector

Sergey Bakhlanov, Nikolay Bazlov, Ilia Chernobrovkin, Denis Danilov, Alexander Derbin, Ilia Drachnev, Irina Kotina, Oleg Konkov, Artem Kuzmichev, Maksim Mikulich, Valentina Muratova, Maxim Trushin,* and Evgeniy Unzhakov

Herein, the investigation of radiation-induced defects generated in the Al/SiO₂/p-type FZ Si surface barrier detector upon irradiation with α -particles at room temperature using capacitance–voltage (C–V) and current deep-level transient spectroscopy (IDLTS) methods is conducted. The carried out C–V measurements indicate the formation of at least $8 \times 10^{12} \text{ cm}^{-3}$ radiation-induced acceptor traps at the depth fairly close to that where, according to TRIM simulations, the highest concentration of vacancy-interstitial pairs is created by the incoming α -particles. The studies conducted by the current DLTS technique allow to relate the observed increase in the acceptor concentration with the near-midgap level at $E_v + 0.56 \text{ eV}$. This level can apparently be associated with V₂O defects recognized previously to be responsible for the space–charge sign inversion in the irradiated n-type Si detectors.

1. Introduction

Unlike most semiconductor electronic devices, the detrimental influence of nuclear radiation on the operational parameters of semiconductor detectors is unavoidable during device application. Incoming radiation not only generates the electron–hole pairs in the detector's sensitive volume, producing thus an information signal, but also causes the destruction of the crystal lattice.^[1–3] Accumulation of the radiation-induced defects reduces the nonequilibrium carrier lifetime and therefore degrades the main operational parameter of the detector—its energy resolution. Most effectively, this process proceeds in case of irradiation by α -particles, accelerated ions, or fission

fragments, which are capable of transferring a significant fraction of their energy to the atoms of the detector lattice. The questions treating the influence of radiation on the detector's characteristics hold an important position in various scientific investigations, as in a number of current and future nuclear physic experiments, semiconductor detectors are forced to operate under the intense level of fission fragments and α -particle irradiation, which inevitably accompanies the spontaneous nuclear fission.^[4,5] Therefore, the studies of the radiation-induced defects and their influence on the detector performance are highly relevant for the successful implementation of these experiments.

The present work is devoted to the investigations of the radiation defects induced in the p-type FZ Si surface barrier detector under irradiation with α -particles by means of the capacitance–voltage (C–V) method and deep-level transient spectroscopy technique working in the current mode (IDLTS). According to the early experimental findings, p-type silicon may be more radiation hard with respect to the n-type silicon, so the investigations of the radiation-induced defects in p-type Si are of a great interest now.^[6,7] The information obtained on the created defect types and density in p-type Si detectors will be essential for the production of the effective radiation hard silicon detectors as well as for other fields of science, where the radiation level is important, as in nuclear reactors, radiotherapy, and space applications.

2. Results

2.1. Characterization of the As-Prepared Detector

Accurate measurements of the depletion capacitance and hence the depletion depth require the capacitive impedance be the dominant circuit element, that is, the fulfillment of the inequality


$$R_s \ll (2\pi f C)^{-1} \quad (1)$$

where R_s is the series resistance of the diode, C is the highest diode capacitance (at zero bias), and f is the capacitance measurement frequency.^[8] Special care should be taken in choosing the proper frequency f for C–V measurements on Si detectors as they are usually produced with a relatively large rectifying contact area (depending on the required active area of the detector) and

S. Bakhlanov, Dr. A. Derbin, Dr. I. Drachnev, Dr. I. Kotina, A. Kuzmichev, M. Mikulich, Dr. V. Muratova, Dr. M. Trushin, E. Unzhakov
 NRC “Kurchatov Institute” Petersburg Nuclear Physics Institute
 mkr. Orlova roshcha 1, 188309 Gatchina, Russia
 E-mail: trushin_mv@pnpi.nrcki.ru

N. Bazlov, D. Danilov
 Department of Physics
 Saint-Petersburg State University
 Universitetskaya nab. 7/9, 199034 St. Petersburg, Russia

Dr. O. Konkov
 Ioffe Physical Technical Institute
 Politekhicheskaya 26, 194021 St. Petersburg, Russia

 The ORCID identification number(s) for the author(s) of this article can be found under <https://doi.org/10.1002/pssa.202100212>.

DOI: 10.1002/pssa.202100212

on high-resistive material (to provide large depletion depth at a moderate applied bias), what implies large C and R_s values, respectively. The series resistance of the investigated detector was estimated from the slope of the forward branch of $I-V$ curve to be about $1.5\text{ k}\Omega$. Therefore, to fulfill the inequality, Equation (1), the capacitance measurement frequency was set at 10 kHz , and the $C-V$ curve measured on the as-prepared detector is shown in **Figure 1**. The profile of shallow acceptors recalculated from this $C-V$ curve revealed flat distribution of acceptor dopants at the level of $5 \times 10^{12}\text{ cm}^{-3}$, what corresponds well with the wafer resistivity; see **Figure 2**. IDLTS measurements on the as-prepared detector did not reveal any deep levels in the active region of the detector where the absorption of α -particles takes place.

2.2. Characterization of the Irradiated Detector

After irradiation, a local increase in the detector capacitance in the range of the reverse biases from 1 to 6 V was detected; see the comparison of $C-V$ curves measured on the as-prepared and

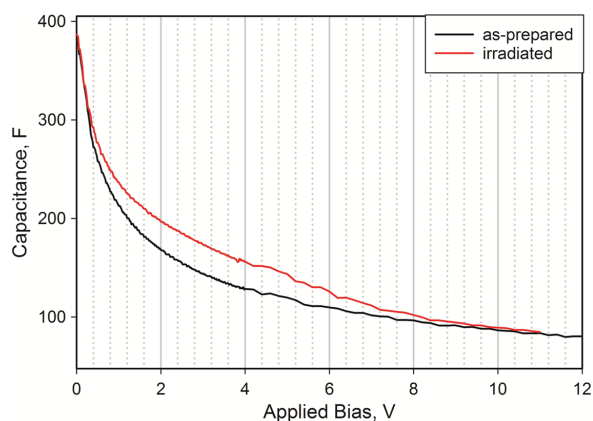


Figure 1. $C-V$ curves measured on the as-prepared and irradiated detector at room temperature. Capacitance measurement frequency was set at 10 kHz .

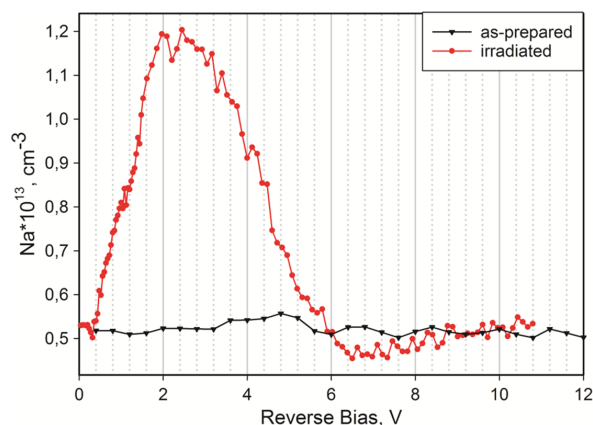


Figure 2. Acceptor distribution profiles in the as-prepared and irradiated detector recalculated from the $C-V$ curves shown in **Figure 1**.

on irradiated detector in **Figure 1**. The corresponding $C-V$ profile revealed a broad peak reaching the value of $1.2 \times 10^{13}\text{ cm}^{-3}$ relative to the doping level of $5 \times 10^{12}\text{ cm}^{-3}$; see **Figure 2**.

Parameters of defect levels introduced into the Si bandgap by α -irradiation were defined by IDLTS measurements. Concentrations of the detected traps were recalculated using the expression describing the magnitude of the IDLTS signal

$$N_t = \frac{2S(T)t_r}{Akq(w_r - w_p)} \quad (2)$$

where $S(T)$ is the temperature-dependent IDLTS signal (in Ampere), t_r is the reference time constant of the rate window, A is the diode area, q is the electron charge, k is the proportionality coefficient, which depends on the exact correlator system (for double box-car correlator $k = 0.363$), and w_r and w_p are the space-charge region (SCR) depths corresponding to the applied reverse bias U_r and the pulse voltage U_p used for the measurements.^[8] For IDLTS peaks appearing at different temperatures, the respective SCR depths were recalculated from capacitance values measured at corresponding temperatures.

Three IDLTS spectra were recorded with different U_r and U_p voltages to determine a possible correlation with the broad acceptor peak appearing on the $C-V$ profile of the irradiated detector. The first spectrum was recorded with the reverse bias voltage $U_r = 5\text{ V}$ and the pulse voltage $U_p = 1\text{ V}$. The voltage range between 1 and 5 V just corresponds to the biases of the acceptor peak appearance in **Figure 2**, so the probing depth during the recordance of this spectrum corresponds to the depth where the defects responsible for the capacitance increase in the irradiated detector are located. As a result, two clearly resolved peaks of considerably different magnitudes were detected at the temperatures near 205 and 280 K, see **Figure 3**. Concentrations of the corresponding traps were estimated, using Equation (2), to be around $6 \times 10^{11}\text{ cm}^{-3}$ and $3 \times 10^{12}\text{ cm}^{-3}$, respectively. The activation enthalpies E_a and capture cross sections were derived from the Arrhenius plots shown in **Figure 4** and the obtained

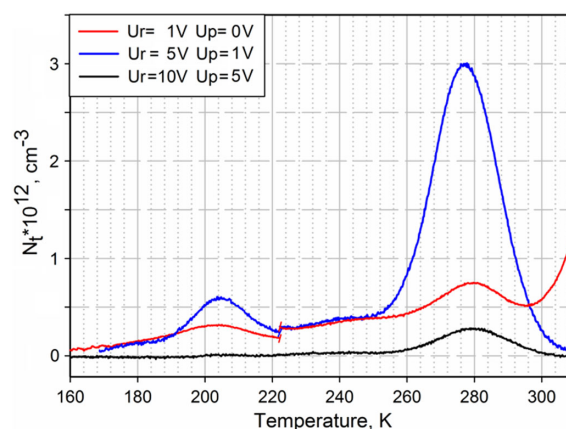


Figure 3. IDLTS spectra recorded with different voltage parameters (see comments in the text), filling pulse durations, and rate window period, 1 ms. The part of the spectra below 220 K was recalculated to represent trap concentration N_t using capacitance values measured at 205 K, whereas above 220 K-using the capacitance values measured at room temperature, respectively.

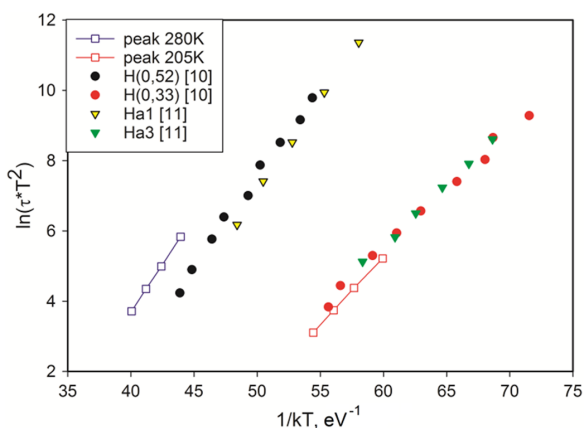


Figure 4. Arrhenius plots for the traps revealed in the irradiated detector (empty squares) in comparison with those ones reported previously in the studies by Danga et al.^[9] (circles) and Mamor et al.^[10] (triangles) for the deep traps in p-type Si samples irradiated by α -particles.

values are 0.38 eV and $5 \times 10^{-14} \text{ cm}^2$ for shallower traps and 0.56 eV and $6 \times 10^{-14} \text{ cm}^2$ for deeper ones.

Another spectrum was recorded with $U_r = 10 \text{ V}$ and $U_p = 5 \text{ V}$, and these voltages according to the $C-V$ profile in Figure 2 exceed the bias range of the broad peak appearance. Only one peak due to the deeper traps at around 280 K remains visible with its magnitude decreasing drastically by nearly one order of magnitude as compared with the previous spectrum.

The third spectrum was recorded with $U_r = 1 \text{ V}$ and $U_p = 0 \text{ V}$ —the biases corresponding to the left shoulder of the broad peak on the $C-V$ profile of the irradiated detector. Both 205 and 280 K peaks were detected, but their magnitudes are considerably lower than that in the first spectrum recorded with $U_r = 5 \text{ V}$ and $U_p = 1 \text{ V}$. An additional signal visible above 300 K occurred due to surface states at the Si/SiO₂ interface and was presented in the spectrum before irradiation. It should be noted also that all IDLTS spectra were measured up to the temperature of 20 K, but no other peaks appearing at the temperature below 200 K were detected.

3. Discussion

Capacitance increase observed on the irradiated detector (Figure 1) implies the formation of a locally distributed radiation-induced acceptor charge in the detector SCR, which is reflected on the $C-V$ profile as a broad peak (Figure 2). The carried out IDLTS measurements (Figure 3) have revealed two defect levels reaching their highest concentration at the same voltages as the acceptor peak on the $C-V$ profile of the irradiated detector, suggesting thus that one of these levels should be of acceptor type responsible for the additional acceptor charge.

Arrhenius plots for these two IDLTS peaks are compared in Figure 4 with those ones reported previously for the deep traps in α -irradiated p-type Si samples.^[9,10] Close coincidence was established between the Arrhenius graph for the 205 K peak with those for H(0.33) and H α 3 peaks, respectively, which were attributed to the interstitial carbon (C_i)-related defects. However,

Arrhenius graph for the 280 K peak seems not to be identical with the Arrhenius graphs for H α 1 and H(0.52) peaks in spite of rather close activation energies—0.56 eV for our peak 280 K and 0.52 eV for H α 1 and H(0.52) peaks, respectively.

The charge state of C_i -related defects was found previously to be $0/+$,^[11] that is, zero when traps are empty and positively charged when filled with holes, so this defect level could not be responsible for the increase of the acceptor charge in our irradiated detector, whereas the exact origin and the charge state of H α 1/H(0.52) defects were not defined, as well as nothing was reported in previous works about the increase of the acceptor charge in α -irradiated p-type Si.^[6,9,10,12]

However, the formation of radiation-induced defects of the acceptor type was frequently observed previously in gamma (proton, pion)-irradiated Si detectors produced on n-type wafers, where it led to gradually inversion of initial n-type conductivity into p-type with the increase in the irradiation dose—the so-called space-charge sign inversion (SCSI) effect.^[1–3,11] As the acceptor defect responsible for charge sign inversion, the so-called I defect tentatively ascribed to the divacancy oxygen complex (V_2O) with its level lying almost at the middle of Si bandgap at 0.55 eV below the conduction band edge was considered.^[11,13]

We thus assume that the radiation-induced acceptor charge in our detector is related with the deeper traps with the activation energy of 0.56 eV, producing the dominating IDLTS peak at 280 K and which could be also ascribed to the V_2O acceptor defects. The reasons for this assumption are the following. 1) I defects were observed predominantly in the irradiated FZ silicon (oxygen lean), whereas in CZ silicon (oxygen reach), their formation is suppressed by a competing reaction with the formation of VO complexes.^[13] Our detector was also made from FZ silicon. 2) V_2O defects were observed in n-type Si after irradiation by gammas, protons, or pions, which similar to alphas introduce mainly point-like defects.^[3,11,13] 3) In the work of Penttilä et al.,^[13] it was shown that the level of I defect can exchange by charge carriers with both conductivity and valence bands, what in DLTS experiments results in the appearance of two peaks with different activation energies of 0.55 eV for the case of electron emission toward the conductivity band and 0.58 eV for holes emission toward the valence band—the latter value is pretty close to the activation energy of 0.56 eV derived for our 280 K IDLTS peak. Then the absence of the radiation-induced acceptor growth in the previous investigations could be related either with CZ silicon type used for the investigations or with a relatively high doping level of the investigated samples in the order of a few 10^{15} cm^{-3} , which made any possible changes in the acceptor concentration at a level of a few 10^{13} cm^{-3} be hardly detectable on $C-V$ profiles.^[6,9,10,12]

The near mid-gap level of I (or V_2O) defect was recognized previously to give the main contribution to the reverse current growth in the irradiated detector.^[11] Similar, the radiation induced increase of the reverse current of the investigated detector (from 0.2 to 0.7 μA at operating reverse bias of 10 V) could be attributed to this near mid-gap level.

In the case when one deep trap level dominates in the sample SCR (namely, the 0.56 eV traps in the investigated detector), its distribution profile can be extracted from the measured $C-V$ curve.^[8] In the neutral region, the defect level with the activation energy of 0.56 eV would lie above the Fermi level (0.4 eV above

the valence band at room temperature in the investigated sample with the doping density of $5 \times 10^{12} \text{ cm}^{-3}$, where it will be filled with holes and thus be of zero charge. However in SCR due to band bending, the trap level crosses the Fermi level at a distance x_1 below the surface and when the applied bias is changed by the step ΔV during the $C-V$ curve measurement, the charge of shallow acceptors would change in the vicinity of the SCR edge w and after a time longer compared with the emission time, the charge of the deep acceptor traps at x_1 . It can be shown then that the charge density derived from $C-V$ curve would represent a sum

$$N(w) = N_a(w) + \frac{x_1}{w} N_t(x_1) \quad (3)$$

where N_a is the doping acceptor density at the SCR edge (which could be considered to be uniform at a level of $5 \times 10^{12} \text{ cm}^{-3}$) and N_t is the deep acceptor trap density at x_1 point.^[8] SCR depth w can be found from the measured capacitance value. Note that the emission rate for these traps being around 1000 s^{-1} at room temperature is less than the angular frequency $2\pi f$ with $f = 10 \text{ kHz}$, implying that these traps could not respond to the small oscillating voltage at the capacitance measurement frequency f , so the high-frequency capacitance is measured and w is derived correctly.^[8] The x_1 distance in the uniformly doped material is equal to^[8]

$$x_1 = w - \lambda = w - \sqrt{\frac{2\epsilon\epsilon_0}{qN_a}(E_t - E_F)} \quad (4)$$

The trap profile $N_t(x_1)$ recalculated from the $C-V$ profile in Figure 3 using Equation (3) and (4) is shown in **Figure 5**, together with the primary vacancies distribution profiles produced by the α -particles of three different energies (4824, 5156, and 5499 keV) in Al/SiO₂/Si structure corresponding to the investigated detector, were calculated by TRIM program (TRAnsport of Ions in Matter).^[14] As shown in Figure 5, the profile of the deep acceptor traps $N_t(x_1)$ represents a peak reaching the value of $8 \times 10^{12} \text{ cm}^{-3}$ at the depth of about 18–20 μm , whereas the region of

highest vacancy production lies somewhat deeper between 20 and 28 μm according to TRIM simulations.

It was shown previously that the distribution profile of the secondary radiation-induced defects remains unbroadened (i.e., the defect diffusion is suppressed) in case of defect generation inside the SCR—as it was in case of the investigated sample.^[15] Therefore we suppose that the discrepancy in vacancies and trap distribution profiles is related with the limited depth resolution of the $C-V$ profiling method. The edge of the depletion region is not abrupt in reality but distributed over 5–7 extrinsic Debye lengths L_D , which in the investigated detector produced on low-doped Si is about $L_D = 1.9 \mu\text{m}$.^[8] This means, first of all, that rapid variations in doping or defect distribution on a depth scale at about L_D could not be reproduced faithfully on a $C-V$ profile.^[8,16] As a result, the deep acceptor profile in Figure 5 represents a broad single peak instead of three separate peaks, as it follows from the simulated vacancies distribution, as the full-width at half-maximum (FWHM) of each vacancy peak and the distance between them is smaller or comparable with L_D . Moreover, it was shown by numerical simulations^[8,16] that the smearing of the SCR edge leads to the shift of the feature on the traps profile derived from the $C-V$ curve relative to the real distribution of the defects by 2–3 Debye lengths, that is by 4–6 μm , what just corresponds to the shift of the calculated defect profile relative to the center of the integrated vacancy profile. Accounting for these factors, the depth distribution of the defect profile recalculated from $C-V$ curve is in a reasonable agreement with the vacancy profiles simulated by TRIM. Discrepancy in the concentration of deep acceptor levels determined from IDLTS and Equation (3) may be related with the fact that the IDLTS method underestimates the concentration of near-midgap levels when the emission rates toward the valence and conduction band are comparable.^[8] Note also that the distribution profile of C_i -related defects seems to be somewhat different from that of deep acceptor defects, as could be concluded from the different ratios of amplitudes of corresponding IDLTS peaks on the spectra measured with the reverse biases of 1 and 5 V, as shown in Figure 3. Additional investigations are needed to clarify this moment.

4. Conclusion

Prolonged room-temperature α -particle irradiation of the p-type FZ Si surface barrier detector with a total fluence of $2 \times 10^{10} \text{ cm}^{-2}$ has led to local increase of the acceptor charge in the SCR of the detector. The increase of the acceptor charge was related with the radiation-induced defect level at 0.56 eV above the valence band, which was detected by IDLTS. Depth distribution of the radiation-induced acceptor defects derived from the $C-V$ measurements was found to correlate well enough (by taking into account the limited accuracy of the $C-V$ profiling method) with that for primary vacancies produced by the incoming α -particles calculated by TRIM. Concentration of the radiation-induced acceptor defects reaches the value of up to $8 \times 10^{12} \text{ cm}^{-3}$.

We suppose that the observed 0.56 eV defect level may be identified with divacancy oxygen V_2O defects detected previously in irradiated FZ n-type silicon, where they were considered to be responsible for SCSi from initial n-type into p-type upon irradiation by introducing an acceptor level in the middle of Si bandgap.

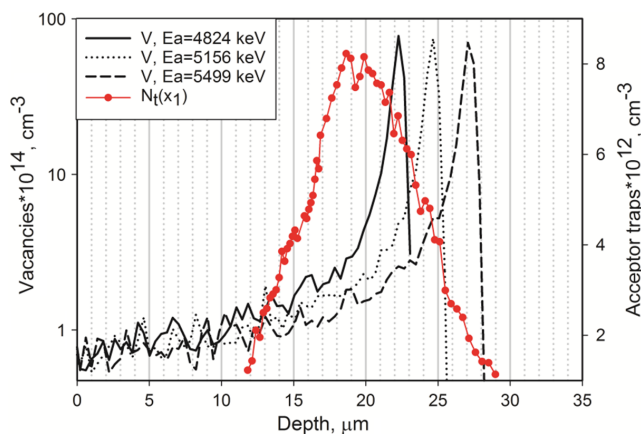


Figure 5. Comparison of the deep traps distribution profile calculated according to Equation (3), with the vacancies distributions calculated by TRIM program for α -particles of three different energies. Note that TRIM does not account for any possible vacancy interaction in the solid including vacancy-interstitial recombination.

Therefore, opposite to n-type Si-based detectors, no SCS effect takes place in α -irradiated p-type FZ Si surface barrier detectors, but the increase in radiation-induced acceptor charge occurs. Finally, we may note that as the types of Si wafers studied in this work are also used as a starting material for SiLi p-i-n detector fabrication, the similar defects may be expected in α -irradiated SiLi detectors as well.

5. Experimental Section

The detector for the experiments was fabricated from a p-type boron-doped silicon wafer of (111) orientation. Diameter of the wafer was 10 mm and resistivity and a carrier lifetime were about $2.5 \text{ k}\Omega \times \text{cm}$ and $1000 \mu\text{s}$, respectively. After mechanical polishing, the wafer was thoroughly cleaned and etched in $\text{HNO}_3\text{:HF}$ (8:1) solution. Afterward, the wafer was oxidized in concentrated boiled HNO_3 solution to produce a thin tunnel transparent oxide layer, which served as a passivation coating (the so-called nitric acid oxidation of Si (NAOS) method).^[17] Ohmic contact was made by evaporation of the Pd layer on the whole rear side of the wafer, whereas the rectifying one by evaporation of Al dot of 7 mm diameter and $\approx 150 \text{ nm}$ thickness in the center of the wafer's front side.

For traps' characterization, SULA DLTS spectroscopy system working in a current transient registration mode was used. The method of IDLTS is especially well suited for traps' investigation in high-resistive samples, where the standard capacitance DLTS method operating usually at a fixed frequency of typically 1 MHz encounters limitations as high series resistance distorts the capacitive measurement (as discussed in Section 2.1).^[8] After routine assessment including current–voltage (I – V), capacitance–voltage (C – V), and IDLTS characterization of the as-prepared detector, it was exposed to α -particle irradiation for 40 days in a vacuum chamber at room temperature. For irradiation, a reference spectrometric triple source containing ^{233}U , ^{239}Pu , and ^{238}Pu isotopes emitting α -particles at 4824, 5156, and 5499 keV with almost equal activities, respectively, was used. The source collimated up to a diameter of 7 mm was placed at a distance of 3 cm above the detector, so the beam of α -particles could be considered to be directed almost perpendicularly toward the detector surface.

Reverse bias voltage applied to the detector during irradiation was set to 10 V, what was proved to be enough to register the spectrum of α -particles (space–charge region depth corresponding to 10 V was around $50 \mu\text{m}$ in our detector, whereas the penetration depth of α -particles in Si was less than $30 \mu\text{m}$), whereas the reverse current remained small. The integrated number of α -particles registered by the detector amounted to 8×10^9 , what corresponded to a fluence Φ of $\approx 2 \times 10^{10} \text{ cm}^{-2}$. Detector reverse current as well as the detector resolution (full-width at half-maximum (FWHM) of α -peaks) were monitored during the whole irradiation period. After irradiation, the detector was subjected to thorough electrical characterization including C – V and IDLTS measurements. A separate article describing the degradation of the operational parameters (resolution, reverse current, etc.) of the investigated p-type Si surface barrier detector under irradiation with α -particles will be published elsewhere.

Acknowledgements

The reported study was funded by RFBR, project number 20-02-00571.

Conflict of Interest

The authors declare no conflict of interest.

Data Availability Statement

The data that support the findings of this study are available from the corresponding author upon reasonable request.

Keywords

deep-level transient spectroscopy, radiation-induced defects, semiconductor detectors, silicon, α -particles

Received: April 15, 2021

Revised: June 4, 2021

Published online:

- [1] M. Moll, *IEEE Trans. Nucl. Sci.* **2018**, 65, 1561.
- [2] Z. Li, *Adv. Mater. Res.* **2013**, 631–632, 216.
- [3] I. Pintilie, G. Lindstroem, A. Junkes, E. Fretwurst, *Nucl. Instr. Methods Phys. Res. A* **2009**, 611, 52.
- [4] C. E. Aalseth, F. Acerbi, P. Agnes, I. F. M. Albuquerque, T. Alexander, A. Alici, A. K. Alton, P. Antonioli, S. Arcelli, R. Ardito, I. J. Arndt, D. M. Asner, M. Ave, H. O. Back, A. I. Barrado Olmedo, G. Batignani, E. Bertoldo, S. Bettarini, M. G. Bisogni, V. Bocci, A. Bondar, G. Bonfini, W. Bonivento, M. Bossa, B. Bottino, M. Boulay, R. Bunker, S. Bussino, A. Buzulutskov, M. Cadeddu, et al., *Eur. Phys. J. Plus* **2018**, 133, 131.
- [5] F. An, G. An, Q. An, V. Antonelli, E. Baussan, J. Beacom, L. Bezrukov, S. Blyth, R. Brugnera, M. B. Avanzini, J. Busto, A. Cabrera, H. Cai, X. Cai, A. Cammi, G. Cao, J. Cao, Y. Chang, S. Chen, S. Chen, Y. Chen, D. Chiesa, M. Clemenza, B. Clerbaux, J. Conrad, D. D'Angelo, H. De Kerret, Z. Deng, Z. Deng, Y. Ding, et al., *J. Phys. G Nucl. Part. Phys.* **2016**, 43, 030401.
- [6] L. F. Makarenko, S. B. Lastovskii, H. S. Yakushevich, M. Moll, I. Pintilie, *J. Appl. Phys.* **2018**, 123, 161576.
- [7] W. Rosenzweig, F. M. Smits, W. L. Brown, *J. Appl. Phys.*, **1964**, 35, 2707.
- [8] P. Blood, J. W. Orton, *The Electrical Characterization of Semiconductors: Majority Carriers and Electron States*, Academic Press Limited, London **1992**.
- [9] H. T. Danga, F. D. Aurret, S. M. Tunhuma, E. Omotoso, E. Igumbor, W. E. Meyer, *Phys. B Condens. Matter* **2018**, 535, 99.
- [10] M. Mamor, M. Willander, F. D. Aurret, W. E. Meyer, E. Sveinbjörnsson, *Phys. Rev. B* **2001**, 63, 452011.
- [11] B. C. MacEvoy, A. Santocchia, G. Hall, *Phys. B* **1999**, 273–274, 1045.
- [12] M. Asghar, M. Z. Iqbal, N. Zafar, *J. Appl. Phys.* **1993**, 73, 4240.
- [13] I. Pintilie, E. Fretwurst, G. Lindström, J. Stahl, *Appl. Phys. Lett.* **2002**, 81, 165.
- [14] J. F. Ziegler, J. P. Biersack, M. D. Ziegler, SRIM – Stopping and Range of Ions in Matter, www.srim.org (accessed: March 2021).
- [15] L. Palmethofer, J. Reisinger, *J. Appl. Phys.* **1992**, 72, 2167.
- [16] C. P. Wu, E. C. Douglas, C. W. Mueller, *IEEE Trans. Electron. Dev.* **1975**, 22, 319.
- [17] H. Kobayashi Asuha, O. Maida, M. Takahashi, H. Iwasa Maida, M. Takahashi, H. Iwasa, *J. Appl. Phys.* **2003**, 94, 7328.